

## Protective Effects of Simultaneous Over-expression of apoA I and SR-B I by AAV2-mediated Gene Transfer in The Atherosclerosis Rat Model\*

LI Bing-Nan<sup>1,2)</sup>, LI Zhi-Yan<sup>1,2)</sup>, ZHANG Juan<sup>1,2)</sup>, LIU Zhen-Qing<sup>1,2)</sup>, TAN Meng-Qun<sup>1,2)\*\*</sup>

<sup>(1)</sup> Experimental Hematology Laboratory, Department of Physiology, Xiangya School of Medicine, Central South University, Changsha 410078, China;

<sup>(2)</sup> Shenzhen Institute of Xiangya Biomedicine, Shenzhen 518057, China)

**Abstract** The adeno-associated virus (AAV) has many safety features that favor its use in the treatment of arteriosclerosis; however, the conventional, adeno-associated virus (AAV) mediated single-gene delivery is inefficient for arteriosclerosis. This has been attributed that the incidence of atherosclerosis is caused by a variety of genetic defects but not a particular gene. To overcome this, double-gene delivery was evaluated for the treatment of atherosclerosis. Four experimental groups were administered the following AAV vector constructs: rAAV-apoA I -IRES-SR-B I, rAAV-apoA I -GFP, rAAV-IRES-GFP, and PBS. ApoA I and SR-B I gene expression was detected using RT-PCR. The apoA I and SR-B I protein expression was determined by Western blotting and ELISA. Diet-induced hypercholesterolemia and atherosclerosis in rats was adopted and rAAV was administered through the tail vein injection. HepG2 cells were cultured and infected with the three viral vectors. The apoA I and SR-B I secreted from HepG2 cells in the AAV- apoA I /SR-B I group enhanced cholesterol efflux and resulted in a stronger RCT ability, respectively. In the rats' model with diet-induced hypercholesterolemia and atherosclerosis, GFP expression could be detected at 8 weeks post-injection. The rAAV vector had superior gene expressing activity. Eight weeks after gene transfer, plasma total cholesterol and LDL-cholesterol concentrations were significantly reduced ( $P < 0.05$ ) compared to control for rAAV-IRES-GFP (AAV-GFP) treated group. No effect on HDL-cholesterol concentrations occurred. Ultrasound determined intima-media thickness also has been significantly reduced compared to control. Serum hs-CRP and SOD levels increased significantly ( $P < 0.01$ ). Serum MDA levels decreased significantly. Gene mRNA expression was detected in atherosclerosis rats' model. The results show that rAAV-hapoA I -IRES-hSR-B I vector can anti-inflammatory, reduce atherosclerotic macrophage content and increases lesion stability of pre-existing plaques through quenching of NF- $\kappa$ B activity and reducing plasma cholesterol. Simultaneous over-expression of apoA I and SR-B I by AAV-mediated gene transfer may have a favorable effect on diet-induced hypercholesterolemia and arteriosclerosis in rats. These results may provide a new method for gene therapy of arteriosclerosis.

**Key words** adeno-associated virus, apolipoprotein A- I, scavenger receptor class B type I, reverse cholesterol transport (RCT), gene therapy

**DOI:** 10.3724/SP.J.1206.2011.00013

Cholesterol efflux is the first step in the reverse cholesterol transport (RCT) pathway, removing excess cholesterol from tissues, including the arterial wall, thus preventing the development of atherosclerosis<sup>[1]</sup>. Enhancing cholesterol efflux from the arterial wall may potentially prevent and even reverse intracellular accumulation of cholesteryl esters, a hallmark of atherosclerosis. Enhancing cholesterol efflux from liver cells, the main source of high density lipoprotein (HDL), raises plasma HDL concentrations<sup>[2]</sup> and consequently increases protection against atherosclerosis

by RCT and other mechanisms<sup>[3]</sup>. Enhanced cholesterol efflux can be achieved either by improving the ability of extracellular acceptors to take up cholesterol released from cells or by stimulating cells to release

\*This work was supported by a grant from Shenzhen Institute of Xiangya Biomedicine.

\*\*Corresponding author.

Tel: 86-755-86142223, E-mail: mqtan26@yeah.net

Received: February 9, 2011 Accepted: March 29, 2011

more cholesterol to plasma acceptors. A number of approaches have been tested to improve the ability of cells to release cholesterol. One of these approaches is overexpression of genes involved in the cholesterol efflux pathways. Overexpression of ABCA1<sup>[4]</sup>, scavenger receptor class B, type I (SR-B I)<sup>[5]</sup>, or sterol 27-hydroxylase (CYP27A1)<sup>[6]</sup> enhances cholesterol efflux *in vitro*. *In vivo* overexpression of the genes for ABCA1<sup>[7]</sup> and SR-B I<sup>[8]</sup> leads to increased protection against atherosclerosis. Stimulation of cholesterol efflux *in vitro* and enhanced protection against atherosclerosis *in vivo* are also achieved by overexpression of several genes involved in lipoprotein metabolism in plasma, but not normally expressed in most extrahepatic cells. These included apoA I<sup>[9-10]</sup>, hormone-sensitive lipase<sup>[11]</sup>, and cholesteryl ester transfer protein<sup>[12]</sup>.

Choosing a safe and effective vector system to transfer and correctly express a target gene during gene therapy is important. Several different strategies have been examined for the delivery of genes of interest, including the use of naked DNA or an adenoviral vector. Treatment with naked DNA is simple and well tolerated by the recipient organism due to its low toxicity and weak induction of immune responses. However, the transduction efficiency is significantly lower when compared with other methods. The adenovirus has frequently been the vector of choice for gene transfer because it is able to transduce a variety of cells with high efficiency. However, adenoviral vectors have major limitations, including a lack of sustained expression, the antigenicity of viral proteins that are targeted by both humoral immunity and cytotoxic T lymphocytes, and possible toxicity at high doses. However, there are many inherent features of the adeno-associated virus system that make it an attractive option as a human viral vector. AAV is a non-pathogenic, defective human parvovirus that requires the presence of a helper virus, such as adenovirus or herpes virus, for productive infection<sup>[13-14]</sup>. Other advantages of this vector system include its low immunogenicity, its ability to transduce both dividing and non-dividing cells, the potential to integrate into specific sites, its ability to achieve long-term gene expression (even *in vivo*), and its broad tropism, allowing for the efficient transduction of diverse organs<sup>[15]</sup>. These features make AAV

attractive and efficient for gene transfer *in vitro* and local injection *in vivo*.

To enhance reverse cholesterol transport during hypercholesterolemia and atherosclerosis therapy, we constructed adeno-associated viruses co-expressing apoA I and SR-B I (rAAV-apoA I -IRES-SR-B I) and detected their effect on gene expression and biological activity *in vitro* and *in vivo*. These data demonstrate the synergistic action of these two genes and may provide a new therapeutic option for hypercholesterolemia and atherosclerosis.

## 1 Methods and materials

### 1.1 rAAV vector production

The construction of the rAAV-apoA I -IRES-SR-B I (AAV-apoA I /SR-B I), rAAV-apoA I -GFP (AAV-apoA I), and rAAV-IRES-GFP (AAV-GFP) vectors was kept in our laboratory. The structure of both rAAV-apoA I -GFP(AAV-apoA I) and pAAV-apoA I -IRES-SR-B I vector is shown in Figure 1. IRES sequences were incorporated into the pAAV MCS to construct a bicistronic vector with two multiple cloning sites. Then, the apoA I and SR-B I genes were inserted into the upstream and downstream MCS, respectively. The length of the bicistronic frame is 2.9 kb, which is within the capacity of the vector. Large quantities of AAV-2 vectors were prepared by using the AAV Helper-Free System (Stratagene). One hundred 100-cm<sup>2</sup> plates of HEK293 cells grown at 80% confluence were cotransfected with recombinant plasmid or the control plasmid pAAV-apoA I -IRES-hrGFP, pHelper and pAAVRC using a calcium phosphate-based protocol. Twenty-four hours later, fresh Dulbecco's minimum essential medium (DMEM) containing 10% newborn calf serum (NBS) was given to transfected HEK293 cells. Cells were collected 70 h after transfection, and rAAV were released from the cells by repeated freezing and thawing. rAAV vectors were purified by single-step column purification (SSCP) of AAV2 by gravity flow based on their affinity to heparin<sup>[16]</sup>. Viral titers were determined by dot-blot analysis. The purity of rAAV-PON1 was determined by sodium dodecyl sulfate polyacrylamide gel electrophoresis (SDS-PAGE). The purified vectors were tested for their infectious ability and transgene expression by infecting HepG2 cells.

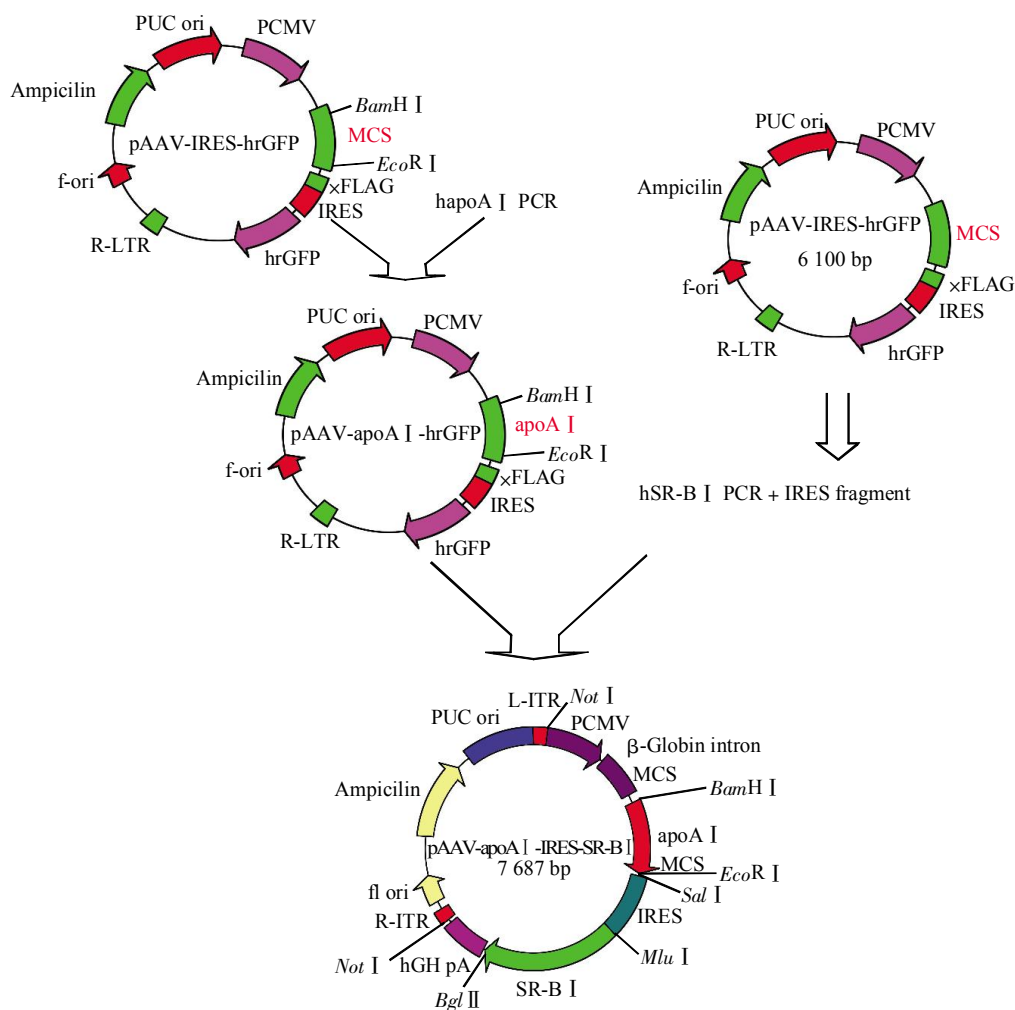


**Fig. 1 Conceptual diagram of construction of pAAV-hapoA I -IRES-hrGFP and pAAV-hapoA I -IRES-SR-B I**

ApoA I gene (804 bp) and SR-B I gene (1 530 bp) were respectively inserted into upstream MCS and downstream MCS located on either side of IRES sequence (670 bp). The length of the bicistronic frame is 2.9 kb.

## 1.2 *In vitro* transduction of HepG2 cells

HepG2 cells were maintained in Dulbecco's modified Essential Medium (DMEM) containing 10% newborn bovine serum (NBS; Hangzhou Sijiqing Biological Products, Hangzhou, China) and 100 mg/L penicillin/streptomycin. Cells were maintained in a humidified environment at 37°C and 5% CO<sub>2</sub>. Cell viability was monitored with trypan blue exclusion method. The viability was over 95% in all experiments. Cells were seeded at a density of 1×10<sup>5</sup> cells/well in a 12-well tissue culture plate and cultured for 24 h to 60% ~ 80% confluence. HepG2 cells were either mock infected or infected with the rAAV-hrGFP, pAAV-apoA I -IRES-hrGFP, and pAAV-apoA I -IRES-SR-B I three vectors respectively for 2 h at 37°C at

5 × 10<sup>4</sup> particles per cell. Two hours later the transfection medium was removed, and fresh complete growth medium was added. Twenty-four hours post-transfection, they were observed under the inverted fluorescent microscope.

## 1.3 The establishment of an AS rat model

Forty male healthy SD rats (200 ~ 300 g) were randomly divided into 5 groups (Table 1), with 8 rats per group. For three months, the control group (A) was fed with basic food, while the other groups were loaded with a high-fat diet. The levels of plasma total cholesterol (TC), triglyceride (TG) and low-density lipoprotein cholesterol (LDL-C) were determined with Biochemical Analyser (Unicel Dxc800, Beckman). The pathological changes of rat aorta were evaluated

*via* ultrasonography after three months high fat diet. All experimental protocols were approved by the Institutional Animal Care and Use Committee of Zhongshan Medical University and conformed to the Guide for the Care and Use of Laboratory Animals published by the National Institutes of Health, China. After three months of dietary treatment, the rats were injected *via* the tail vein with either vehicle, rAAV-IRES-hrGFP vectors ( $1 \times 10^{10}$  v.g./1 ml PBS), rAAV-apoA I -IRES-hrGFP vectors ( $1 \times 10^{10}$  v.g./1 ml PBS) or rAAV-apoA I -IRES-SR-B I vectors ( $1 \times 10^{10}$  v.g./1 ml PBS) (as shown in Table 1). After transplantation, all animals were fed with basic food and survived the experiments.

**Table 1 Experimental group**

Group	Treatment
A control	PBS (1 ml)
B untreated	rAAV-IRES-hrGFP( $1 \times 10^{10}$ v.g./1ml PBS)
C apoA I	rAAV-apoA I -IRES-hrGFP( $1 \times 10^{10}$ v.g./1ml PBS)
D apoA I /SR-B I	rAAV-apoA I -IRES-SR-B I ( $1 \times 10^{10}$ v.g./1ml PBS)

#### 1.4 Tissue collection and preparation

Animals were sacrificed by the intravenous injection of potassium chloride at two months after cell transplantation. The abdominal aorta and liver were harvested and divided into two parts. One part of these tissues was used for cryosectioning. The other part was snap-frozen in liquid nitrogen and stored at  $-80^{\circ}\text{C}$  for RT-PCR and Western blot analysis.

#### 1.5 mRNA analysis by RT-PCR

To detect the mRNA expression levels in aortas and liver. For RT-PCR analysis, 500 ng of RNA was used for the RT-PCR reaction in a volume of 25  $\mu\text{l}$  using gene specific primers and primers for an internal control, which was  $\beta$ -actin. PCRs were done for cycles each consisting of  $94^{\circ}\text{C}$  for 30 s,  $56^{\circ}\text{C}$  for 30 s, and  $72^{\circ}\text{C}$  for 1 min. The primers used for  $\beta$ -actin were: forward, 5' AGCGGGAAATCGTGCGTGAC 3'; reverse, 5' CAAGAAAGGGTGTAACGCAACTA 3'. The sequences of primers for detecting apoA I and SR-B I were as follows: apoA I forward, 5' CGCG-GATCCATGAAAGCTGCGGTGCTGAC 3'; apoA I reverse, R-apoA1, 5' CCGGAATTCTCACTGGGT-GTTGAGCTTC 3'; SR-B I forward, 5' TTAAC-CGCGTATGGGCTGCTCCGCCAAAGC 3'; SR-B I reverse, 5' GCGCAGATCTCTACAGTTTTGCTTCC-

TGCAGC 3'.

#### 1.6 Protein analysis by Western blotting and ELISA

A standard Western blotting protocol was used to detect SR-B I protein expression in liver. The same amount of protein extracted from liver was separated on SDS-PAGE under reducing and denaturing conditions and transferred to Hybond nitrocellulose membranes. The membranes were incubated in a 1 : 400 dilution of polyclonal rabbit anti-SR-BI antibody (Abcam), followed by incubation with horseradish peroxidase-conjugated secondary antibody (1 : 2 000, Santa-Cruz).  $\beta$ -Actin (1 : 400, Santa-Cruz) was used as the loading control. Peroxidaseconjugated affinipure sheep anti- rabbit immunoglobulin G (IgG) was used as secondary antibody (Beijing Zhongshan Golden Bridge Biotechnology Co, Ltd, China). Proteins were detected by means of DAB color kit (Santa Cruz Biotechnology, USA). The amount of signal was quantified with a scanning laser densitometer (Molecular Dynamics, Sunnyvale, CA). Western blotting was performed on a sample of all animals in each group and at least twice for each animal. At 8 weeks post-injection, we measured the apolipoprotein A I concentration in rats' serum by enzyme-linked immunosorbent assay (ELISA) according to the manufacturer's instructions. Each assay was performed in triplicate.

#### 1.7 Detection of Doppler ultrasound and the levels of serum lipids

Two months after the transplantation, the condition of atherosclerosis in the aorta was evaluated with Doppler ultrasound. The rats were anesthetized with an intraperitoneal injection of 10% chloral hydrate. Three separate measurements were done for each rat, and the results were averaged. Two months after the transplantation, the levels of serum lipids were evaluated.

#### 1.8 Determined the changes of atherosclerosis-related genes expression

Inflammation plays an important role in all stages of atherosclerosis, but little is known about the therapeutic effects of quenching inflammation in already existing atherosclerotic lesions. We used rAAV as a gene transduction system by successfully inserting the apoA I and SR-B I genes in this vector, allowing them to be efficiently and stably co-expressed to determine whether it can inhibit the NF- $\kappa$ B activation which was studied in rat with established

lesions. We determined the changes of some atherosclerosis-related genes expression in aortas after transplantation, NF- $\kappa$ Bp65, I $\kappa$ B $\alpha$ , eNOS, VCAM-1, ICAM-1, IL-1 $\beta$ , MCP-1, MMP-2 and MMP-9 expression was primarily assessed by means of RT-PCR. The methods of extracting total RNA and reverse transcription were same as the above. PCR amplification of these sequences from harvested cDNAs used these primers: NF-KBp65 primer1 (forward), 5' ATGGACGATCTGTTTCCCCT 3' and primer2 (reverse), 5' GGTGCGTCTTAGTGGTATCT 3'; I $\kappa$ B $\alpha$  primer 3 (forward), 5' CCTCAACTCCAGAACAACCTG 3' and primer4(reverse), 5' GGCGTAATAGGTGTAATG 3'; eNOS primer5 (forward), 5' GACCCTCACCGATACAACATAC 3' and primer6 (reverse), 5' GCTCACGGATAGCACTCACACA 3'; VCAM-1 primer7(forward), 5' TAAGTTCACAGCAGTCAAATGGA 3' and primer8 (reverse), 5' CACATACATAAATGCCGGAATCTT 3'; ICAM-1 primer9 (forward), 5' AGACACAAGCAAGAGAA-GAA 3' and primer10(reverse), 5' GAGAAGCCCA-AACCCGTATG 3'; IL-1 $\beta$  primer11(forward), 5' TGTGACTCGTGGGATGATGAC 3' and primer12 (reverse), 5' GTCGTTGCTTGTCTCTCCTTG 3'; MCP-1 primer13 (forward), 5' CTCACCTGCTGCTACTCATTC 3' and primer14 (reverse), 5' CTC-TGTCATACTGGTCACTTCTAC 3'; MMP-2 primer15 (forward), 5' ACCGTCGCCCATCATCA-AGT 3' and primer16 (reverse), 5' CCATCTCC-ATTGCCACCCAT 3'; MMP-9 primer17 (forward), 5' GACGGTCGGTATTGGAAGTTC 3' and primer18 (reverse), 5' TCACACGCCAGAAGTATTTGTC 3'; Rat  $\beta$ -actin primer 19 (forward), 5' AGCGGGA-AATCGTGCGTGAC 3' and primer 20 (reverse), 5' CAAGAAAGGGTGTAACGCAACTA 3'. PCR was performed using the following program: 94°C for 3 min for 1 cycle and 35 cycles at 94°C for 30 s, 55°C for 30 s, and 72°C for 45 s. The PCR products were electrophoresed on ethidium bromide-stained 2.0% agarose gels. Each assay was performed in triplicate.

### 1.9 Determination of serum hs-CRP, MDA, SOD levels

Two months after the transplantation, vessel bloods were collected for plasma hs-CRP, MDA and SOD measurement. The plasma MDA and the SOD activity were measured using chemical assay kits (Nanjing Jiancheng Biological Product, Nanjing, China). MDA levels were estimated by thiobarbituric

acid (TBA) reaction. The results were expressed as  $\mu$ mol/ml and U/ml, respectively. Multiple prospective studies in the US and Europe have confirmed that Hs-CRP is an independent predictor of future cardiovascular disease<sup>[17]</sup>. High Sensitive CRP (Hs-CRP) levels were determined with ELISA method. All assays were performed in duplicate or triplicate for each specific sample.

### 1.10 Statistical analysis

Results are expressed as  $\bar{x} \pm s$ . Comparisons between groups were analyzed by a one-way ANOVA.  $P < 0.05$  were considered statistically significant. All analyses were performed with SPSS 13.0 software.

## 2 Results

### 2.1 Establishment of the AS rat model

After 3 months of high fat diet feeding, the rats developed atherosclerotic plaques on aorta. The plasma levels of TC, and LDL-C levels of high-fat diet rats were significantly higher than those of normal-diet rats at 3 months after giving the high-fat diet ( $*P < 0.01$ , Table 2).

**Table 2 The level of serum lipid of high-fat diet rat in the third month**

Group	TC	LDL-C	HDL-C	TG
A	2.34 $\pm$ 1.52	0.33 $\pm$ 0.11	1.47 $\pm$ 0.42	1.04 $\pm$ 0.38
B	8.16 $\pm$ 2.07*	2.35 $\pm$ 0.74*	2.70 $\pm$ 0.39	0.69 $\pm$ 0.35
C	7.93 $\pm$ 1.11*	2.40 $\pm$ 1.55*	2.59 $\pm$ 0.27	0.55 $\pm$ 0.19
D	7.54 $\pm$ 2.12*	2.19 $\pm$ 0.90*	2.75 $\pm$ 0.41	0.93 $\pm$ 0.54

\* $P < 0.01$  vs control group. A: Normal diet B, C and D: High-fat diet.

After 3 months of high fat diet feeding, the condition of atherosclerosis in the aorta was observed with Doppler ultrasound. In the control group, the aortic tunica intima of rats was slicking, and there was no thickening or plaque on the vessel wall(Figure 2b-1). The ultrasound changes of atherosclerosis were found in the aorta of rats in the untreated group (Figure 2b-2), including increased intima-media thickness and a rough and discontinuous intima. The small hyperechoic spot showed the existence of plaque (Figure 2b-2). Comparison of IMT showed a significant difference ( $*P < 0.01$ ), between normal diet group and high diet group after three months feeding (Figure 2c).

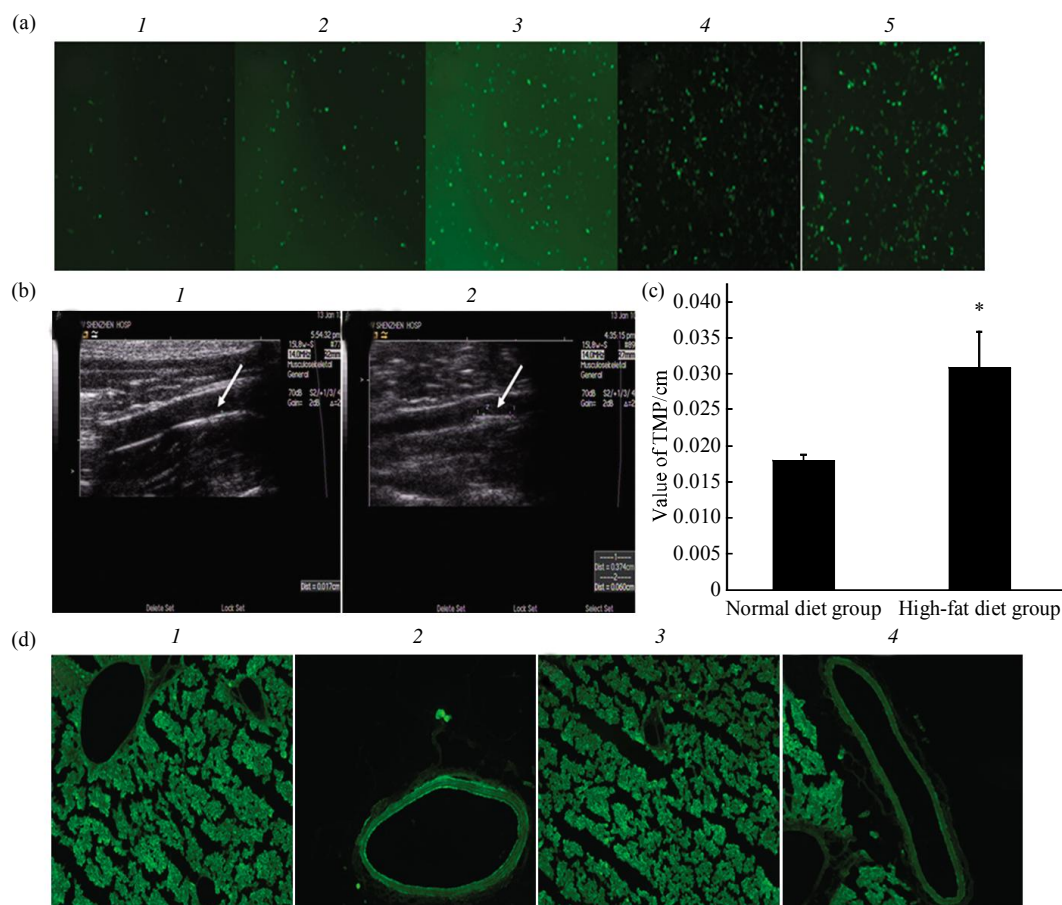


**Fig. 2 Representative images of GFP protein expression**

(a) Effect of various AAV vector particles per HepG2 cell. AAV vector particles per cell, respectively, are shown: 1:  $10^2$ ; 2:  $10^3$ ; 3:  $10^4$ ; 4:  $10^5$ ; 5:  $10^6$ . (b) The ultrasonic testing of the rat artery. 1: The rat artery of control group; 2: The rat artery of the high-fat diet group. (c) Comparison of IMT between normal diet group and high diet group after three months feeding. \* $P < 0.01$  vs normal diet group. (d) Fluorescence photomicrograph of rat carotid artery and liver frozen sections. 1: Liver GFP expression in AAV-GFP; 2: GFP-expressing vessel in AAV-GFP group; 3: Liver GFP expression in AAV-apoA I; 4: GFP-expressing vessel in AAV-apoA I group.

## 2.2 The effects of various particles per cell of rAAV vectors on transduction of HepG2 cells

We measured the transduction efficiency of HepG2 cells infected with  $1 \times 10^2 \sim 1 \times 10^6$  rAAV-apoA I particles per cell. There was a dose-dependence between the AAV vector particles per cell and transduction efficiency within a certain range (Figure 2a). When AAV vectors were used at concentration of  $1 \times 10^5$  per cell, transduction efficiency was more than 70%.

## 2.3 Efficient genes expression of hapoA I and hSR-B I

To confirm hapoA I and hSR-B I gene expression *in vivo*, RT-PCR assays were performed. As shown in Figure 3a and b, the sizes of the PCR products for apoA I, SR-B I, and  $\beta$ -actin were 804 bp, 1 530 bp,

and 551 bp, respectively. These data demonstrate that apoA I was expressed in the AAV-apoA I and AAV-apoA I /SR-B I groups but not in the control and AAV-GFP groups and that SR-B I was expressed in the AAV-apoA I /SR-B I group but not in the control, AAV-apoA I and AAV-GFP groups. Protein expression of 8 weeks following injection with AAV-apoA I /SR-B I *in vivo* is shown in Figure 3c, d. Expression of the SR-B I was visualized by Western blot analysis. Strong staining at the expected molecular mass of 82 ku (SR-B I) and 43 ku ( $\beta$ -actin) was observed. These data demonstrate that SR-B I was expressed in the AAV-apoA I /SR-B I group but not in the control, AAV-GFP and AAV-apoA I groups. As shown in Figure 3e, the production of hapoA I was quantified in the serum of rats 8 weeks post-injection

by ELISA assay. The average amounts of protein in the AAV-apoA I /SR-B I and AAV-apoA I groups were significantly higher than those in the control

and AAV-GFP groups ( $*P < 0.01, n = 12$ ). GFP protein expression could be detected at 8 weeks post-infection (Figure 2d).

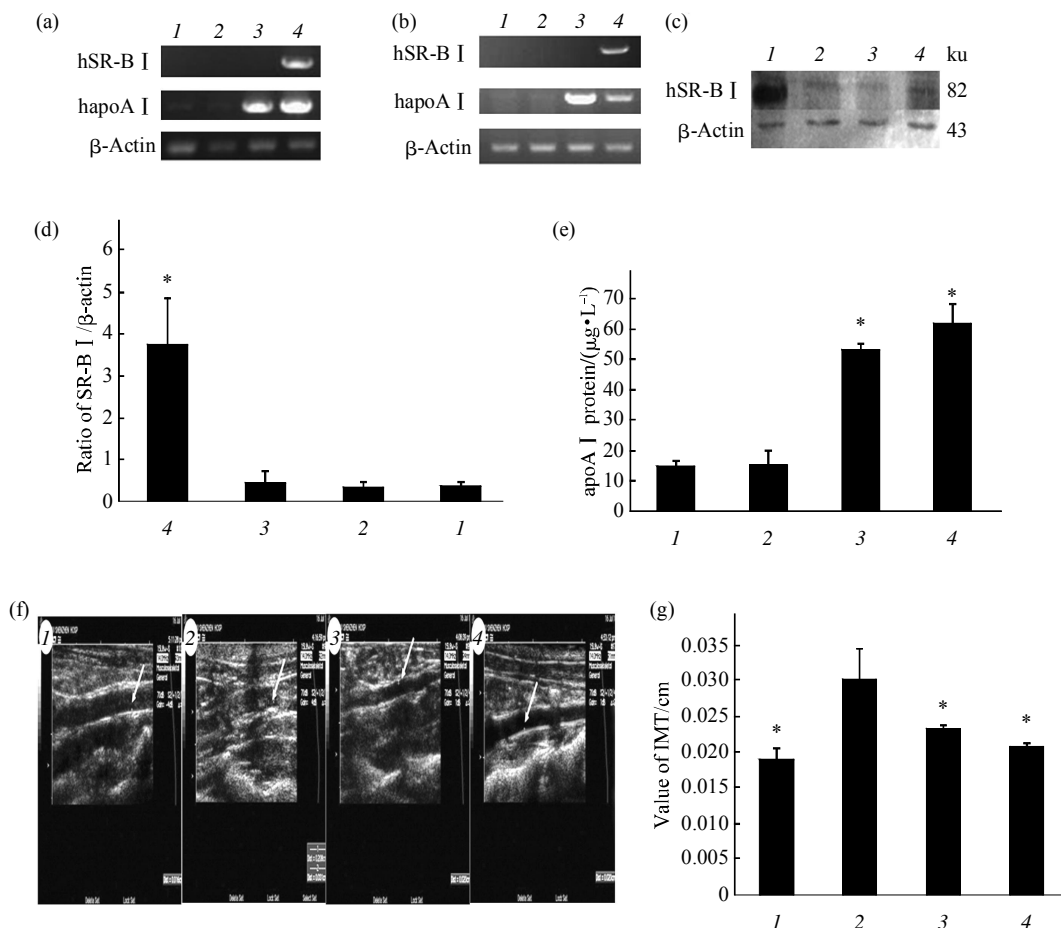


**Fig. 3 Expression of hapoA I and hSR-B I**

(a) Transgene mRNA expression in the aorta. (b) Transgene mRNA expression in the liver. (c) Western blot analysis of SR-B I expression 2 months after the transplantation. The liver samples were homogenized and processed for Western blotting using an anti-SR-B I antibody. This was performed using  $\beta$ -actin as an internal standard. (d) Suggesting that exogenous SR-B I was strongly expressed in the AVV-apoA I /SR-B I group. 1: Control group; 2: AAV-GFP; 3: AAV-apoA I ; 4: AAV- apoA I /SR-B I group;  $*P < 0.01$  vs group B. (e) Transgene apoA I expression in the serum.  $*P < 0.01$  vs. control and AAV-GFP. 1: Control group; 2: AAV-GFP; 3: AAV-apoA I ; 4: AAV- apoA I /SR-B I . (f) Ultrasound of the rat aorta. 1: Control group (group A); 2: Untreated group (group B); 3: AAV-apoA I -treated group (group C); 4: AAV-apoA I -IRES-hrGFP treated group(group D). (g) Comparision of IMT after gene transfer for two months among the control group, AAV-GFP group, AAV-apoA I group and AAV-apoA I /SR-B I group.  $*P < 0.05$  vs. AAV-GFP treated group. 1: Control group; 2: AAV-GFP; 3: AAV-apoA I ; 4: AAV- apoA I /SR-B I .

**2.4 Detection by Doppler ultrasound**

Two months after the transplantation, the condition of atherosclerosis in the aorta was observed with Doppler ultrasound. In the control group, the aortic tunica intima of rats was slicking, and there was no thickening or plaque on the vessel wall(Figure 3f-1). The ultrasound changes of atherosclerosis were found in the aorta of rats in the untreated group (Figure 3f-2), including increased intima-media thickness and a rough and discontinuous intima. The small hyperechoic

spot showed the existence of plaque (Figure 3f-2). There was no obvious plaque in the aortic tunica intima of rats in every treated group. Comparision of IMT after gene transfer for two months among the control group, AAV-GFP group, AAV-apoA I group and AAV-apoA I /SR-B I group (Figure 3g).  $*P < 0.05$  vs. AAV-GFP treated group.

**2.5 Atherosclerosis-related genes mRNA expression in aorta**

The atherosclerosis-related genes NF- $\kappa$ Bp65,

ICAM-1, VCAM-1, IL-1 $\beta$ , MCP-1, MMP-2, MMP-9, mRNA level on the aortic in AAV-GFP group was higher than that in AAV-apoA I /SR-B I group, AAV-GFP group and control group (\* $P < 0.01$ ) (Figure 4a, c, d, f, g, h, i) while the atherosclerosis-

related genes I $\kappa$ B $\alpha$ , eNOS in AAV-GFP group were significantly lower than those in AAV-apoA I /SR-B I group, AAV-GFP group and control group ( $P < 0.01$ , Figure 4b, e).

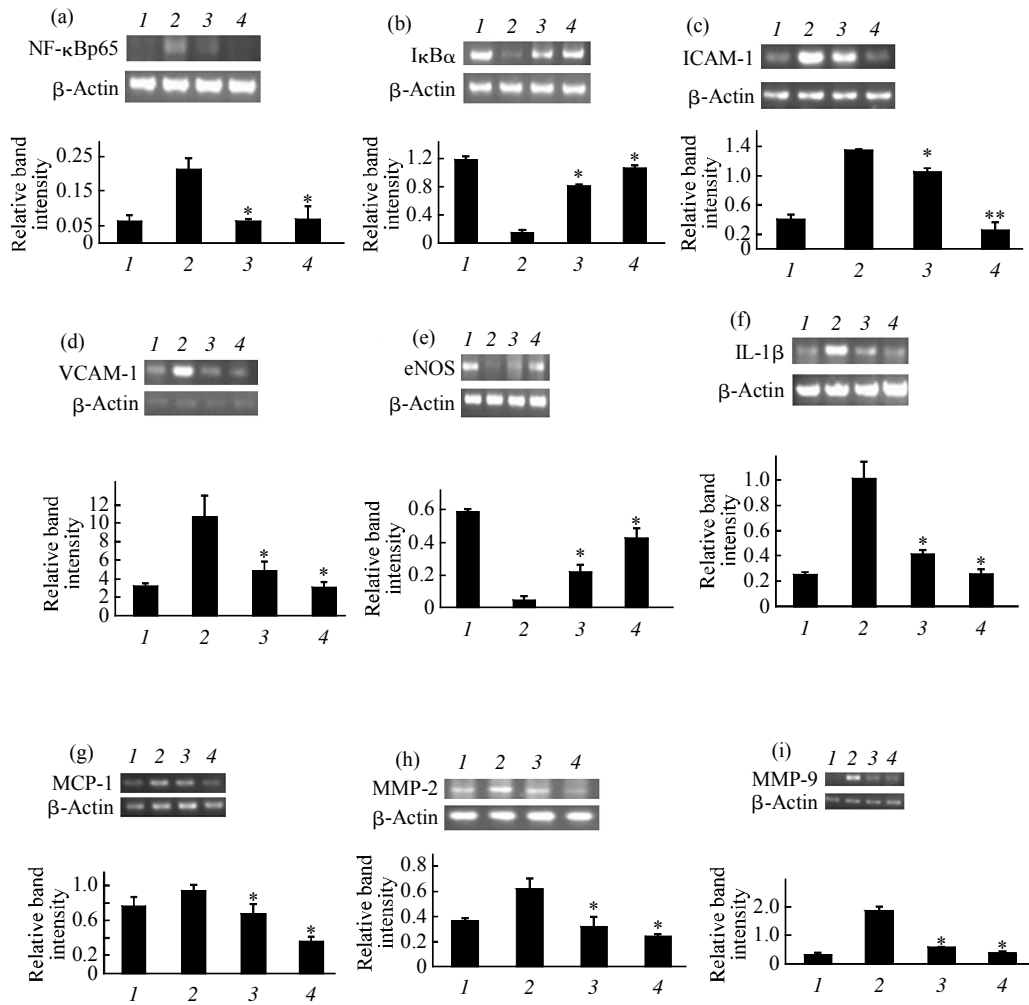


**Fig. 4 The effects on the aortic gene expression two months after the transplantation**

(a) The expression of NF- $\kappa$ Bp65 mRNA by RT-PCR. The size of the PCR products for NF- $\kappa$ Bp65 and  $\beta$ -actin was 175 bp, and 551 bp, respectively. The correspondence absorbance ratio of NF- $\kappa$ Bp65/ $\beta$ -actin. \* $P < 0.01$  vs. group B. (b) The expression of I $\kappa$ B $\alpha$  mRNA by RT-PCR. The size of the PCR products for I $\kappa$ B $\alpha$  and  $\beta$ -actin was 600 bp, and 551 bp, respectively. The correspondence absorbance ratio of I $\kappa$ B $\alpha$ / $\beta$ -actin. \* $P < 0.01$  vs. group B. (c) The expression of ICAM-1 mRNA by RT-PCR. The size of the PCR products for ICAM-1 and  $\beta$ -actin was 283 bp, and 551 bp, respectively. The correspondence absorbance ratio of ICAM-1/ $\beta$ -actin. \* $P < 0.01$  vs. group B. (d) The expression of VCAM-1 mRNA by RT-PCR. The size of the PCR products for VCAM-1 and  $\beta$ -actin was 283 bp, and 551 bp, respectively. The correspondence absorbance ratio of VCAM-1/ $\beta$ -actin. \* $P < 0.01$  vs. group B. (e) The expression of eNOS mRNA by RT-PCR. The size of the PCR products for eNOS and  $\beta$ -actin was 461 bp, and 551 bp, respectively. The correspondence absorbance ratio of eNOS/ $\beta$ -actin. \* $P < 0.01$  vs. group B. (f) The expression of IL-1 $\beta$  mRNA by RT-PCR. The size of the PCR products for IL-1 $\beta$  and  $\beta$ -actin was 201 bp, and 551 bp, respectively. The correspondence absorbance ratio of IL-1 $\beta$ / $\beta$ -actin. \* $P < 0.01$  vs. group B. (g) The expression of MCP-1 mRNA by RT-PCR. The size of the PCR products for MCP-1 and  $\beta$ -actin was 348 bp, and 551 bp, respectively. The correspondence absorbance ratio of MCP-1/ $\beta$ -actin. \* $P < 0.01$  vs. group B. (h) The expression of MMP-2 mRNA by RT-PCR. The size of the PCR products for MMP-2 and  $\beta$ -actin was 774 bp, and 551 bp, respectively. The correspondence absorbance ratio of MMP-2/ $\beta$ -actin. \* $P < 0.01$  vs. group B. (i) The expression of MMP-9 mRNA by RT-PCR. The size of the PCR products for MMP-9 and  $\beta$ -actin was 442 bp, and 551 bp, respectively. The correspondence absorbance ratio of MMP-9/ $\beta$ -actin. \* $P < 0.01$  vs. group B. 1: Control group; 2: AAV-GFP group; 3: AAV-apoA I group; 4: AAV-apoA I /SR-B I group.

### 2.6 The detection of the level of serum lipid two months after the transplantation

Data results have been listed in Table 3. The plasma TC in control group and AAV-apoA I /SR-B I group were significantly lower than those in

AAV-GFP group ( $*P < 0.05$ ) while the plasma LDL-C in AAV-GFP group was higher than that in AAV-apoA I /SR-B I group, AAV-GFP group and control group ( $*P < 0.05$ ).

**Table 3 The level of serum lipid in the second month after treatment**

Group	TC	LDL-C	HDL-C	TG
Control	1.51 ± 0.15	0.20 ± 0.01	0.89 ± 0.32	1.24 ± 1.40
AAV-GFP	2.85 ± 0.78	0.47 ± 0.19	1.56 ± 0.44	1.46 ± 1.10
AAV-apoA I	2.52 ± 0.42	0.20 ± 0.05	1.60 ± 0.32	1.95 ± 0.81
AAV-apoA I /SR-B I	2.11 ± 0.25	0.24 ± 0.05	1.44 ± 0.19	1.23 ± 0.84

\* $P < 0.05$  vs. group B.

### 2.7 Determination of serum hs-CRP, MDA, SOD levels

Data results have been listed in Table 4. The plasma hs-CRP and MDA in AAV-apoA I group and AAV-apoA I /SR-B I group were significantly lower

than those in AAV-GFP group ( $*P < 0.01$ ) while the plasma SOD in AAV-apoA I group and AAV-apoA I /SR-B I group was higher than that in AAV-GFP group ( $*P < 0.01$ ).

**Table 4 The detection of serum hs-CRP, SOD and MDA levels in each group after treatment**

Group	hs-CRP/( $\mu\text{g}\cdot\text{L}^{-1}$ )	SOD/( $\text{U}\cdot\text{ml}^{-1}$ )	MDA/( $\mu\text{mol}\cdot\text{L}^{-1}$ )
Control	27.20 ± 3.25	157.82 ± 9.54	4.10 ± 0.77
AAV-GFP	86.04 ± 5.50	65.32 ± 9.92	18.46 ± 2.56
AAV-apoA I	54.36 ± 4.83*	112.36 ± 6.74*	10.41 ± 1.48*
AAV-apoA I /SR-B I	32.76 ± 4.26**	138.38 ± 6.03**	6.26 ± 2.74**

\* $P < 0.01$  vs. AAV-GFP, \*\* $P < 0.01$  vs. AAV-apoA I.

## 3 Discussion

The packaging capacity of the rAAV vector (5 kb, including the inverted terminal repeats) remains one of its primary limitations in terms of gene delivery. However, substantial progress has recently been made to overcome this restriction. Among the several different strategies to co-express multiple genes, the incorporation of an IRES into this gene therapy vector represents one of the more promising strategies [18-20]. The IRES functions as a ribosome landing pad for the efficient internal initiation of translation, ensuring coordinated expression of several genes. The IRES initiates ribosome binding and translation in the absence of a 5'CAP, thus overcoming the main disadvantage of traditional strategies that

express two different genes. This characteristic is especially useful for AAV production due to the packaging size limitation imposed by the AAV vectors. In our current study, an IRES sequence was incorporated into the pAAV MCS to construct a bicistronic vector. Then, the hapoA I and hSR-B I genes were inserted upstream and downstream of the MCS, located on either side of the IRES to create a bicistronic frame of 2.9 kb in length, which is within the capacity of the vector. In our study, we reveal that AAV-mediated hapoA I and hSR-B I gene transfer *in vitro* and *in vivo* induces the expression and secretion of the hapoA I and hSR-B I proteins. These results demonstrate that the IRES sequence may be a superior strategy for co-expressing multiple genes in rAAVs. An important characteristic of rAAV is that

when the host cell is infected with rAAV, the efficiency of infection cannot immediately be determined. The expression of the gene of interest will not be activated until the double-stranded nucleic acid version of the virus has been synthesized by DNA synthetase. The time required for this to occur may be several days, weeks, or months and is dependent on the infection surrounding the host cells<sup>[21]</sup>. For this reason, it is essential to detect the timing of gene expression *in vitro* and *in vivo*. The results of GFP expression and RT-PCR analysis *in vivo* and of Western blotting and ELISA assays *in vivo* revealed expression of the genes of interest, indicating that the rAAV vector has superior gene expressing ability.

The key aim of gene therapy for diet-induced hypercholesterolemia and atherosclerosis disease is lipid lowering and plaque regression<sup>[22]</sup>. Reverse cholesterol transport (RCT) is a complicated process involving many kinds of factors<sup>[23]</sup>. Scavenger receptor class B, type I (SR-B I) or apoA- I play important roles during cholesterol efflux that have been studied extensively<sup>[24]</sup>. Cholesterol efflux is the first step in the reverse cholesterol transport (RCT) pathway, removing excess cholesterol from tissues, including the arterial wall, thus preventing the development of atherosclerosis<sup>[25]</sup>. The previous studies have confirmed that over expression of scavenger receptor class B, type I (SR-B I) or apoA I *in vitro* and *in vivo* enhances cholesterol efflux which leads to increased protection against atherosclerosis<sup>[26]</sup>. Thus, orchestrating the timing of expression of these two factors may greatly enhance this process.

We performed cholesterol efflux assays to identify the biological effect of hapoA I and hSR-B I *in vitro* and *in vivo*. The results indicated that at the dosage used, the rAAV-hapoA I -IRES-hSR-B I virus had excellent biological activity and could properly mediate biological activity both *in vitro* and *in vivo*. However, one interesting finding of our study was that hapoA I alone or hSR-B I alone is not sufficient to improve cholesterol efflux. We conclude that these findings were not due to improper dosage, but reflect the fact that expression of apoA I or SR-B I alone is not sufficient to initiate the cascade of reverse cholesterol transport, respectively. These findings also demonstrate that orchestrating the expression of these two factors is essential for effective therapy of diet-induced hypercholesterolemia and atherosclerosis

disease. An additional interesting finding in our studies was that there was no statistical difference between the AAV-apoA I /SR-B I group and the AAV-apoA I group in terms of HDL-C and TG. Similarly, there was no statistical difference between the AAV-apoA I /SR-B I group and the AAV-apoA I group in terms of intima-media thickness.

We conclude that there may be a requirement for the proper ratio of apoA I to SR-B I. As shown by a previous study<sup>[27]</sup>, the proper ratio of two related gene is critical to ensure synergistic effects. In addition, the unequal expression of the apoA I and SR-B I genes located upstream and downstream of the IRES may be responsible<sup>[28]</sup>. Thus, comparison of the expression of genes located upstream and downstream of the IRES and the identification of the best ratio of apoA I and SR-B I for treatment of diet-induced hypercholesterolemia and atherosclerosis will be imperative in future experiments. But there was significant statistical difference between the AAV-apoA I /SR-B I group, the AAV-apoA I group, AAV-GFP group and control in terms of serum hs-CRP, MDA, and SOD levels. Similarly, there was significant statistical difference between the AAV-apoA I /SR-B I group, the AAV-apoA I group, AAV-GFP group and control in terms of atherosclerosis-related genes mRNA expression in aorta.

In summary, Inflammation plays an important role in all stages of atherosclerosis, but little is known about the therapeutic effects of quenching inflammation in already existing atherosclerotic lesions. We used rAAV as a gene transduction system by successfully inserting the apoA I and SR-B I genes in this vector, allowing them to be efficiently and stably co-expressed. The apoA I and SR-B I proteins that were expressed from the rAAV-hapoA I - IRES-hSR-B I vector enhanced reverse cholesterol transport *in vitro* and *in vivo*. It can inhibit the NF- $\kappa$ B activation, was studied in rat with established lesions. Our experiments show that rAAV-hapoA I -IRES-hSR-B I vector has anti-inflammatory effect, reduces atherosclerotic macrophage content and increases lesion stability of pre-existing plaques through quenching of NF- $\kappa$ B activity and reducing plasma cholesterol. Our experiments also establish a foundation for investigating the synergistic biological effects of apoA I and SR-B I *in vitro* and *in vivo* and

provide theoretical support for gene therapy of diet-induced hypercholesterolemia and atherosclerosis with our recombinant virus.

### Reference

- [1] Sviridov D, Nestel P. Dynamics of reverse cholesterol transport: protection against atherosclerosis. *Atherosclerosis*, 2002, **161**(2): 245–254
- [2] Basso F, Freeman L, Knapper C L, *et al.* Role of the hepatic ABCA1 transporter in modulating intrahepatic cholesterol and plasma HDL cholesterol concentrations. *J Lipid Res*, 2003, **44**(1): 296–302
- [3] Barter P, Kastelein J, Nunn A, *et al.* High density lipoproteins (HDLs) and atherosclerosis; the unanswered questions. *Atherosclerosis*, 2003, **168**(2): 195–211
- [4] Oram J F, Lawn R M, Garvin M R, *et al.* ABCA1 is the cAMP-inducible apolipoprotein receptor that mediates cholesterol secretion from macrophages. *J Biol Chem*, 2000, **275**(3): 34508–34511
- [5] Ji Y, Jian B, Wang N, *et al.* Scavenger receptor BI promotes high density lipoprotein-mediated cellular cholesterol efflux. *J Biol Chem*, 1997, **272**(34): 20982–20985
- [6] Escher G, Krozowski Z, Croft K D, *et al.* Expression of sterol 27-hydroxylase (CYP27A1) enhances cholesterol efflux. *J Biol Chem*, 2003, **278**(13): 11015–11019
- [7] Joyce C, Freeman L, Jr Brewer H B, *et al.* Study of ABCA1 function in transgenic mice. *arterioscler. Thromb Vasc Biol*, 2003, **23**(1): 965–971
- [8] Ueda Y, Gong E, Royer L, *et al.* Relationship between expression levels and atherogenesis in scavenger receptor class B type I transgenics. *J Biol Chem*, 2000, **275**(27): 20368–20373
- [9] Major A S, Dove D E, Ishiguro H, *et al.* Increased cholesterol efflux in apolipoprotein A I (ApoA I) —Producing macrophages as a mechanism for reduced atherosclerosis in ApoA I<sup>(e)</sup> mice. *arterioscler. Thromb Vasc Biol*, 2001, **21**(1): 1790–1795
- [10] Ishiguro H, Yoshida H, Major A S, *et al.* Retrovirus-mediated expression of apolipoprotein A- I in the macrophage protects against atherosclerosis *in vivo*. *J Biol Chem*, 2001, **276**(39): 36742–36748
- [11] Okazaki H, Osuga J-I, Tsukamoto K, *et al.* Elimination of cholesterol ester from macrophage foam cells by adenovirus-mediated gene transfer of hormone-sensitive lipase. *J Biol Chem*, 2002, **277**(35): 31893–31899
- [12] Zhang Z, Yamashita S, Hirano K, *et al.* Expression of cholesteryl ester transfer protein in human atherosclerotic lesions and its implication in reverse cholesterol transport. *Atherosclerosis*, 2001, **159**(1): 67–75
- [13] Merten O W, Gény-Fiamma C, Douar A M. Current issues in adeno-associated viral vector production. *Gene Ther*, 2005, **12**(1): S51–61
- [14] Grieger J C, Choi V W, Samulski R J. Production and characterization of adeno-associated viral vectors. *Nat Protoc*, 2006, **1**(1): 1412–1428
- [15] Tu L, Xu X, Wan H, *et al.* Delivery of recombinant adeno-associated virus-mediated human tissue Kallikrein for therapy of chronic renal failure in rats. *Hum Gene Ther*, 2008, **19**(4): 318–330
- [16] Auricchio A, Hildinger M, O'Connor E, *et al.* Isolation of highly infectious and pure adeno-associated virus type 2 vectors with a single-step gravity-flow column. *Hum Gene Ther*, 2001, **12**(1): 71–76
- [17] Li Q X, Fu Q Q, Shi S W, *et al.* Relationship between plasma inflammatory markers and plaque fibrous cap thickness determined by intravascular optical coherence tomography. *Heart*, 2010, **96**(1): 196–201
- [18] Pelletier J, Sonenberg N. Internal initiation of translation of eukaryotic mRNA directed by a sequence derived from poliovirus RNA. *Nature*, 1988, **334**(1): 320–325
- [19] Li W, Thakor N, Xu E Y, *et al.* An internal ribosomal entry site mediates redox-sensitive translation of Nrf2. *Nucl Acids Res*, 2009, **38**(3): 778–789
- [20] Kieft J S. Viral IRES RNA structures and ribosome interactions. *Trends Biochem Sci*, 2008, **33**(6): 274–283
- [21] Tang X, Fu D H, Yang S H, *et al.* Assessment of the expression profile during the entochondrostosis of vascular endothelial growth factor in bone morphogenetic protein 2 induced osteogenesis. *Chin J Surgery*, 2008, **46**(8): 614–617
- [22] de Vries-van der Weijab J, Toeta K, Zadelara S, *et al.* Anti-inflammatory salicylate beneficially modulates pre-existing atherosclerosis through quenching of NF-κB activity and lowering of cholesterol. *Atherosclerosis*, 2010, **213**(1): 241–246
- [23] Illiana M, Miranda V E, Theo J C V B. High-density lipoprotein: Key molecule in cholesterol efflux and the prevention of atherosclerosis. *Curr Pharm Design*, 2010, **16**(13): 1445–1467
- [24] Al-Jarallah A, Trigatti B L. A role for the scavenger receptor, class B type I in high density lipoprotein dependent activation of cellular signaling pathways. *Bba-Mol Cell Biol L*, 2010, **1801**(12): 1239–1248
- [25] Hu Y W, Wang Q, Ma X, *et al.* TGF-β1 Up-regulates expression of ABCA1, ABCG1 and SR-BI through liver X receptor α signaling pathway in THP-1 macrophage-derived foam cells. *J Atheroscler Thromb*, 2010, **17**(5): 493–502
- [26] Sviridov D, Nestel P. Dynamics of reverse cholesterol transport: protection against atherosclerosis. *Atherosclerosis*, 2002, **161**(2): 245–254
- [27] Peng H, Wright V, Usas A, *et al.* Synergistic enhancement of bone formation and healing by stem cell-expressed VEGF and bone morphogenetic protein-4. *J Clin Invest*, 2002, **110**(6): 751–759
- [28] Kaptureczak M, Zolotukhin S, Cross J, *et al.* Transduction of human and mouse pancreatic islet cells using a bicistronic recombinant adeno-associated viral vector. *Mol Ther*, 2002, **5**(2): 154–160

## 2 型腺相关病毒载体介导的 apoA I 和 SR-B I 双 基因表达对动脉硬化模型鼠保护效应的研究 \*

栗炳南<sup>1, 2)</sup> 李志艳<sup>1, 2)</sup> 张 娟<sup>1, 2)</sup> 刘珍清<sup>1, 2)</sup> 谭孟群<sup>1, 2)\*\*</sup>

(<sup>1)</sup>中南大学湘雅医学院血液生理系, 长沙 410078; <sup>2)</sup>深圳市湘雅生物医药研究院, 深圳 518057)

**摘要** 重组腺相关病毒载体(AAV)具有很多安全方面的特性, 有利于其在动脉硬化方面的治疗研究. 尽管如此, 传统的介导单个基因的治疗效果并不是很理想, 这都归因于动脉硬化疾病的发生是由于多种基因的缺陷而不是单单某一特定基因. 为了克服这个问题, 尝试了重组腺相关病毒载体介导的双基因对动脉硬化的治疗研究. 实验大鼠分为动脉硬化模型鼠和正常饮食组(即正常对照组), 动脉硬化组大鼠被随机分为 3 组, 分别进行 AAV-apoA I /SR-B I, AAV-apoA I, 与 AAV-GFP 尾静脉注射, 同时正常饮食组尾静脉注射 PBS 作为对照. 其中目的基因 mRNA 检测采用 RT-PCR 方法, 蛋白质表达的检测采用 Western blotting 和 ELISA. 由饮食诱导的动脉硬化和高胆固醇的大鼠模型在尾静脉注射后 8 周进行冰冻切片的荧光检测. 重组 AAV 载体显示出较强的表达活性. 尾静脉注射治疗 8 周后, AAV-apoA I /SR-B I 与 AAV-apoA I 治疗组血浆总胆固醇和低密度脂蛋白胆固醇浓度与 AAV-GFP 治疗组相比有了明显下降( $P < 0.05$ ), 高密度脂蛋白胆固醇浓度各组之间没有明显差异, 彩色多普勒超声检测发现, AAV-apoA I /SR-B I 与 AAV-apoA I 治疗组的腹主动脉的内中膜厚度相对于 AAV-GFP 治疗组有了明显下降( $P < 0.05$ ), 血清 hs-CRP 和 SOD 的水平有了明显上升( $P < 0.01$ ), 血清 MDA 的水平有了明显的下降( $P < 0.01$ ). 同时也检测了动脉硬化相关基因 mRNA 水平的表达. 结果显示, rAAV-hapoA I -IRES-hSR-B I 治疗后可能是通过抑制 NF- $\kappa$ B 的活性发挥抗炎作用减少炎症因子的释放, 增加动脉硬化板块的稳定性以及降低血浆胆固醇含量的. 总之, 利用 2 型腺相关病毒载体介导的基因转移过度表达人载脂蛋白 A I 和 SR-B I 可能对饮食诱发大鼠高胆固醇血症和动脉硬化的产生有利影响. 这些结果可能为动脉粥样硬化基因治疗提供了一种新的研究思路.

**关键词** 2 型腺相关病毒载体, 载脂蛋白 A I, B 族 I 型清道夫受体, 胆固醇逆向转运, 基因治疗

**学科分类号** R54

**DOI:** 10.3724/SP.J.1206.2011.00013

\* 深圳湘雅生物医药研究院资助项目.

\*\* 通讯联系人.

Tel: 0755-86142223, E-mail: mqtan26@yeah.net

收稿日期: 2011-02-09, 接受日期: 2011-03-29